longer time scales can be observed in the 3 months of images now available. For example, there have been two periods, lasting several weeks, during which the Y feature was not apparent even though some of its component parts were present. Bow-shaped features (*4, 5*), which often play an important role in the appearance of the Y feature, have generally been present. The Y feature was absent when the pair of images shown in Fig. 2 were obtained. These images show the morning quadrant approximately 1 month before the series in Fig. 1 and the evening quadrant 1 month after it. The earlier image exhibits bow shapes near the morning terminator, obviously farther upstream from the subsolar point than in Mariner 10 images. The entire 3-month sequence shows small cellular features throughout the low latitudes and occasionally at latitudes as high as ~50°.

The examination and categorization of the ultraviolet cloud features and their evolution is but the first, modest step in attempting to characterize the basic dynamical state of the upper atmosphere and its interaction with the cloud physics. Interpretation of the cloud patterns must be made cautiously because of their diffuse nature (*6*) and the uncertainty regarding the nature of the absorbing and scattering material responsible for the features. At least three different cloud materials contribute to the appearance of the images: (i) an optically thin, high-altitude haze of submicron aerosols (*1*), which is most prevalent near the morning terminator and polar regions; (ii) the diffuse sulfuric acid smog of 1-μm droplets composing the main visible cloud (*7*); and (iii) the ultraviolet absorber located within or below the main visible region of sulfuric acid droplets (*1*). It is possible to define the nature and distribution of these different aerosols more precisely from analysis of polarization measurements obtained by the cloud photopolarimeter. Other key aids are provided by the wind velocities implied by the displacement of small-scale cloud features in successive images and spectral analyses of cloud brightness. These analyses are in progress.

L. D. TRAVIS, D. L. COFFEEN
A. D. DEL GENIO, J. E. HANSEN
K. KAWABATA, A. A. LACIS
W. A. LANE, S. S. LIMAYE
W. B. ROSSOW
NASA Goddard Institute for Space Studies, Goddard Space Flight Center, New York 10025
P. H. STONE
Department of Meteorology, Massachusetts Institute of Technology, Cambridge 02139

References and Notes

1. The initial imaging and polarimetry results were described by L. D. Travis, D. L. Coffeen, J. E. Hansen, K. Kawabata, A. A. Lacis, W. A. Lane, S. S. Limaye, P. H. Stone, *Science* **203**, 781 (1979).
2. Contrast enhancement was performed with high-pass spatial filtering, with scales larger than about 20 percent of the disk diameter excluded. The images presented here are a linear combination of the original data and the high-pass-filtered version, weighted to reveal both the small- and large-scale features.
3. The time given is spacecraft event time in universal time. Phase angle is the angle between the sun-planet and planet-spacecraft directions. The latitudes listed are celestial latitudes, that is, measured from a plane parallel to the ecliptic. The images are oriented with the north pole at the top such that cloud motions from right to left correspond to the retrograde circulation.
4. We use the terminology "bow-shaped features" in the sense of curved or bent, rather than "bowlike waves" (*5*) in the sense of waves generated by the bow of a ship. A term based on morphology rather than on an implicit physical interpretation seems preferable in view of the uncertainty regarding origin of these features.
5. B. C. Murray *et al.*, *Science* **183**, 1307 (1974); M. J. S. Belton, G. R. Smith, D. A. Elliott, K. Klaasen, G. E. Danielson, *J. Atmos. Sci.* **33**, 1383 (1976); M. J. S. Belton, G. R. Smith, G. Schubert, A. D. Del Genio, *ibid.*, p. 1394.
6. K. Kawabata and J. E. Hansen, *J. Atmos. Sci.* **32**, 1133 (1975); A. A. Lacis, *ibid.*, p. 1107.
7. J. E. Hansen and J. W. Hovenier, *ibid.* **31**, 1137 (1974).
8. D.L.C. and W.A.L. were supported by NASA grant 33-015-165 to State University of New York at Stony Brook. A.D.D. and S.S.L. are NASA-NRC resident research associates.

15 May 1979

Nature of the Ultraviolet Absorber in the Venus Clouds: Inferences Based on Pioneer Venus Data

Abstract. *Several photometric measurements of Venus made from the Pioneer Venus orbiter and probes indicate that solar near-ultraviolet radiation is being absorbed throughout much of the main cloud region, but little above the clouds or within the first one or two optical depths. Radiative transfer calculations were carried out to simulate both Pioneer Venus and ground-based data for a number of proposed cloud compositions. This comparison rules out models invoking nitrogen dioxide, meteoritic material, and volatile metals as the source of the ultraviolet absorption. Models involving either small (~ 1 micrometer) or large (~ 10 micrometers) sulfur particles have some serious difficulties, while ones invoking sulfur dioxide gas appear to be promising.*

Beginning at a wavelength of about 0.52 μm, the spherical albedo of Venus steadily declines from a value close to unity to a value of about 0.4 at 0.3 μm (*1*) (Fig. 1). Because clouds totally envelop the surface and are optically thick, this reduction in reflectivity toward the ultraviolet (UV) must be due to some atmospheric component located within or above the main cloud layer. Variations in the properties of the UV-absorbing agent, such as its location with respect to the cloud tops, are believed to be responsible for the marked contrast shown by Venus at wavelengths below about 0.4 μm (*1, 2*).

Strong evidence suggests that concentrated sulfuric acid droplets are the dominant cloud-particle species near the tops of the main cloud deck (*3*), and more limited evidence indicates that it is also present in significant amounts throughout the main cloud layer (*4*). Sulfuric acid is transparent in the blue and near-UV (*5*), however, and so is not the UV-absorbing agent. It has been suggested that the sulfur-containing gases, which serve as precursors for the sulfuric acid particles, might also give rise to elemental sulfur particles and that the sulfur particles are the UV-absorbing agent (*2, 6*). Assuming that the sulfur particles are about 10 μm in size and that they are located only below an optical depth of several, Young (*2*) has obtained a quantitative fit to the wavelength de-

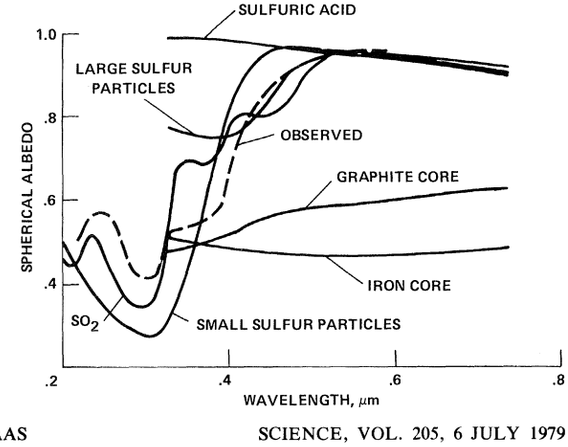

Fig. 1. Comparison of the observed spectral dependence of the spherical albedo of Venus (*1*) and the predicted behavior of several models.

0036-8075/79/0706-0076$00.50/0

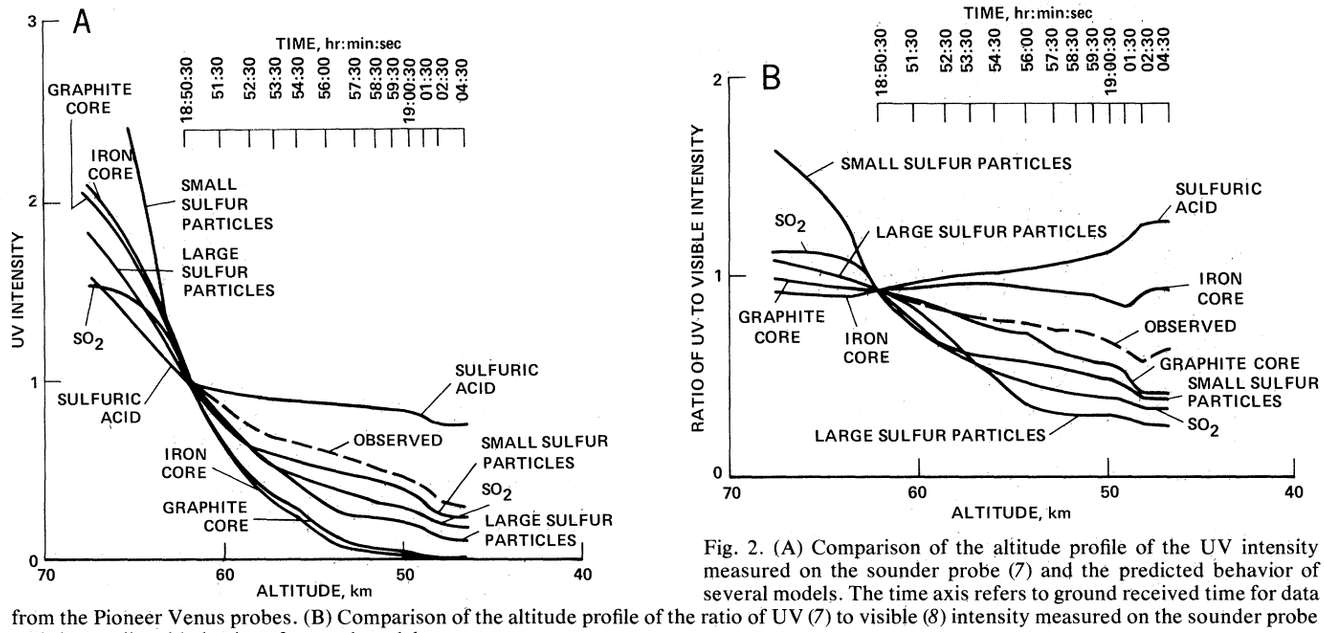

Fig. 2. (A) Comparison of the altitude profile of the UV intensity measured on the sounder probe (*7*) and the predicted behavior of several models. The time axis refers to ground received time for data from the Pioneer Venus probes. (B) Comparison of the altitude profile of the ratio of UV (*7*) to visible (*8*) intensity measured on the sounder probe and the predicted behavior of several models.

pendence of the spherical albedo of Venus and the contrast between bright and dark features.

We have analyzed photometric observations of Venus taken from the Pioneer Venus probes and orbiter and relevant ground-based data to improve significantly our knowledge about the vertical distribution and identity of the UV-absorbing agent. Such information has relevance for the chemistry of Venus's lower atmosphere, its vertical temperature structure in the vicinity of the clouds, and its dynamical regime (through improved interpretation of UV pictures).

Photometric measurements made by several Pioneer Venus probe experiments have helped to define the nature of the UV absorber at altitudes of about 62 km and lower (cloud optical depth, $\gtrsim 4$), and photometric observations obtained by several Pioneer Venus orbiter experiments have provided constraints at higher altitudes. The probe nephelometer experiment included two photometers, which viewed Venus skylight in the UV ($\sim$ 0.3 to 0.4 μm) and visible (0.45 to 0.6 μm) ranges, although both had minor near-infrared light leaks (*7*). Because of the spinning of the probe, a full suite of azimuthal angles are swept out in a fraction of a minute. Figure 2A shows the azimuthally averaged intensity for the UV photometer aboard the sounder probe as a function of altitude throughout the main cloud region. Because of present uncertainties in the absolute calibration, the data have been normalized to a value of 1 at 62 km. The ratio of the intensity in the UV channel to that in the visible channel for the day probe is shown in Fig. 3. Unfortunately, the visible photometer aboard the sounder probe was saturated in the cloud region.

Additional information on the brightness of the sky at the position of the sounder probe is given by the solar flux radiometer experiment (*8*), whose measurements included a determination of the net flux (Fig. 4) and the specific intensity in five directions in a broadband visible channel (0.4 to 1.0 μm). Figure 2B exhibits the ratio of the azimuthally averaged intensity of the nephelometer's UV channel to the solar flux experiment's broadband visible intensity for similar viewing conditions (85.5° versus 83.5° from the upward vertical). Again, because of calibration uncertainties, this ratio profile has been normalized to 1 at 62 km, while the net flux results of Fig. 4 have been normalized to 1 at 60 km.

The cloud photopolarimeter experiment has taken daily pictures of Venus in the near UV ($\sim$ 0.35 μm) from the time of orbit insertion (*9*). During this time interval, the phase angle has decreased from about 120° to 30°. As discussed earlier (*9*) and shown in greater detail in Fig. 5, the contrast between bright and dark regions shows a marked increase with decreasing phase angle. In constructing this figure, the maximum intensity in either of the bright polar rings was compared with the nearest planetary scale local minimum in intensity. Some of the scatter in the data is due to real day-to-day variations in Venus's appearance, and some may be due to difficulties connected with the operational definition of contrast. Additional information about the UV absorber is provided by the limb darkening observations obtained by the UV spectrometer experiment aboard the orbiter, which were obtained at several

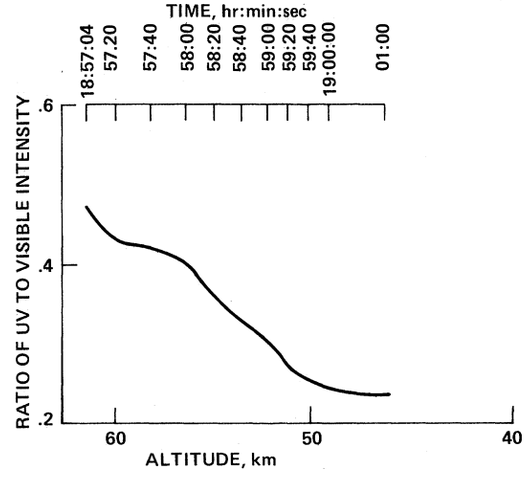

Fig. 3. Altitude profile of the ratio of UV to visible intensity measured on the day probe (*7*).

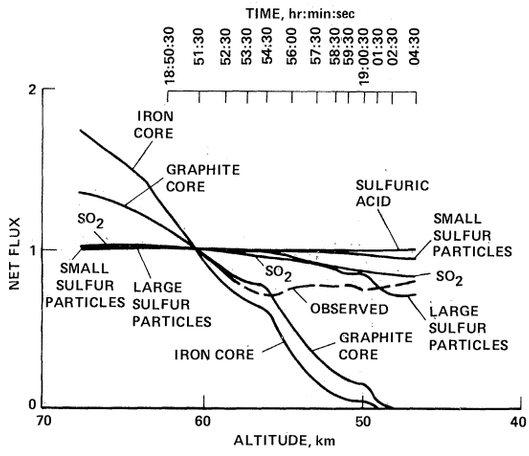

Fig. 4 (left). Comparison of the altitude profile of visible net flux measured on the sounder probe (*8*) and the predicted behavior of several models. Fig. 5 (right). Phase angle dependence of the contrast between UV dark and bright features, as measured from the Pioneer Venus orbiter (*9*).

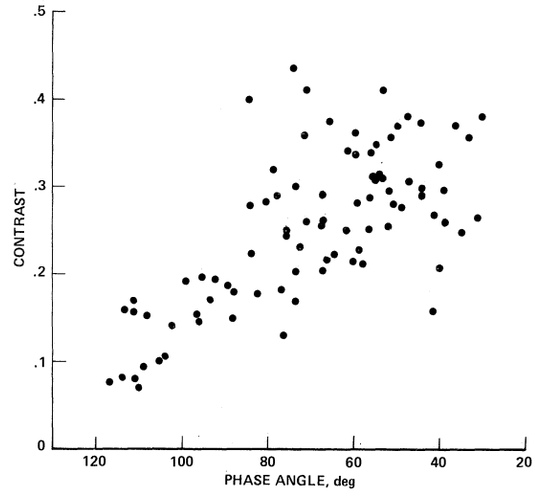

wavelengths between 0.2 and 0.35 μm [figures 1 and 2 of (*10*)].

Ground-based data also place some useful constraints on the properties of the UV absorber. Figure 1 illustrates the wavelength dependence of the planet's spherical albedo. Whereas significant absorption is implied by Fig. 1 in the 0.4- to 0.5-μm spectral region, measurable contrast between dark and bright features occurs only below 0.4 μm. It has been suggested that the difference is due to the vertically inhomogeneous distribution of the UV absorber, with its concentration increasing dramatically in the top few optical depths (*2*). Finally, polarization observations imply that almost all the particles ($\geq$ 80 percent) at optical depth unity are spherical with a refractive index equal to that of concentrated sulfuric acid (*11*).

We briefly considered the qualitative implications of the data for the location of the UV absorber. The variation of contrast with phase angle (Fig. 5) rules out the possibility that the UV absorber lies above the sulfuric acid cloud tops (*9*). Furthermore, analysis of the UV spectrometer's limb-darkening curves suggests that the concentration of the UV absorber increases significantly in the top few optical depths (*10*), in accord with the above-mentioned interpretation of the difference in the spectral characteristics of contrast and albedo. The profiles of the ratios of UV to visible light (Figs. 2B and 3) imply that UV absorption is occurring throughout most of the cloud, but Fig. 4 suggests that absorption at somewhat longer wavelengths occurs in the upper part of the clouds (optical depth, $\lesssim$ 15). The absence of visible absorption at lower altitude could in part be an artifact of the broadband nature of the filter used, with the shorter wavelength portion being removed at high altitude.

In order to refine the conclusions about the location of the UV absorber and to test proposed candidate materials, we simulated the Pioneer Venus data as well as the spherical albedo data (Fig. 1) with a radiative transfer computer program that provides a numerically accurate solution of the multiple scattering problem (*12*). Allowance is made for the vertically inhomogeneous cloud structure, for the possible presence of several aerosol species at a given level, and for scattering and absorption by gases. The single scattering properties of the cloud particles were calculated with a standard Mie scattering program in the case of spherical particles (*12*) and a newly devised method in the case of nonspherical ones (*13*). The size distribution and optical depth profile at the sounder probe location were obtained from the results of (*14*). We assumed that there was an optical depth of several ($\sim$ 4) between the top of the atmosphere and an altitude level of 62 km, which is close to the highest point sampled by most of the probe instruments. Such a choice is qualitatively consistent with the strong damping of the azimuthal dependence of the sky brightness below an altitude of 62 km (*7, 8*).

We considered five candidates for the UV absorber: elemental sulfur (*2*), meteoritic (*14*) and metallic particles, and nitrogen dioxide (*15*) and sulfur dioxide gases. The sulfur particles were assumed to constitute alternatively the largest size mode of the middle and lower clouds (large sulfur particles) and the smallest size mode, which occurs throughout the clouds (small sulfur particles) (*8, 14*). The absorbing component of meteoritic material is dominated by carbonaceous matter, magnetite, and metallic iron. The first was approximated by the properties of graphite. The meteoritic material was assumed to be present as small inclusions or cores uniformly dispersed throughout the sulfuric acid cloud particles, with its fractional abundance ($\sim 10^{-3}$ to 10^{-4}) chosen to yield the observed albedo near 0.32 μm. The properties of metallic iron were also taken as representative of those of metals that could evaporate at the high surface temperature of Venus and recondense at higher altitudes. We also considered a model containing only concentrated sulfuric acid to illustrate the behavior of an almost totally nonabsorbing cloud. The optical constants of concentrated sulfuric acid were obtained from (*5*); those of sulfur from (*16*), with allowance for their temperature dependence from (*2*); and those of graphite, magnetite, and metallic iron from (*17, 18, 19*), respectively. The absorption coefficients of NO_2 and SO_2 were obtained from (*20-22*). The SO_2 mixing ratio profile was constrained to agree with the abundances found near the cloud tops ($\sim 10^{-7}$ at 40 mbar, with a scale height of 1 km) (*10*) and that measured below the clouds ($\sim 2 \times 10^{-4}$) (*23*).

Figures 1 to 4 show the results of the comparisons between the predicted behavior of the models and the observed properties of Venus. We can readily rule out the meteoritic, volatile metal, and NO_2 models. The absorption coefficient of graphite and iron vary only slowly with wavelength and hence are incapable of reproducing the sharp increase in Venus's albedo from 0.4 to 0.5 μm (Fig. 1). For the same reason, the graphite and iron core models exhibit too great a decrease in the UV intensity and net flux within the cloud region, in comparison with the observed behavior (Figs. 2A and 4). Magnetite behaves in a similar manner to graphite. Hence, none of the opaque phases of meteoritic material nor any combination of these phases can lead to an acceptable fit to the observations (*24*). Metallic iron is reasonably

representative of other metals in the wavelength dependence of its absorption coefficient (*19*). Thus, the volatile-metal model for the UV absorber can also be dismissed. The absorption coefficient of NO_2 peaks near 0.4 μm and has similar values at 0.31 and 0.52 μm (*20*). Such a spectral dependence is inconsistent with the wavelength behavior of Venus's spherical albedo.

We next considered models involving elemental sulfur. The small sulfur particle model has several attractive features. Its predicted behavior follows fairly closely the shape and magnitude of the observed UV intensity of Fig. 2A. Also, at first glance, the spherical albedo for this model seems similar to the observed curve. Unfortunately, there are a number of fundamental problems. Its spherical albedo decreases very sharply from 0.4 to 0.32 μm, in marked contrast to the observed behavior. This failure results from a combination of a sharp increase in the absorption coefficient of sulfur with decreasing wavelength and from the presence of sulfur particles in significant amounts in the upper cloud region. Also, mode 1 contributes at least 35 percent and more likely in excess of 50 percent to the extinction cross section at altitudes around 60 km (*8, 14*). It is difficult to find a simple mechanism that will diminish the relative abundance of these small particles to values ($\lesssim$ 20 percent) near optical depth unity that are consistent with the polarization constraints discussed earlier. Finally, this model produces too little absorption of light longward of 0.4 μm from the top of the cloud to its bottom and only a negligible amount above 55 km, where the net flux decreases by the largest amount (Fig. 4). This inconsistency is due to the inability of ordinary sulfur to absorb above 0.4 μm at the relatively cold temperatures of the upper cloud region and to mode 1's being a minor component of the lower cloud regions.

The large sulfur particle model also has problems. The spherical albedo is too high in the 0.3- to 0.4-μm spectral domain. However, if the optical depth of the upper cloud region—from which mode 3 is missing—is smaller for the planet as a whole than at the sounder probe location, this problem would be rectified. This model does produce an approximately correct shape to the albedo curve in the 0.32- to 0.4-μm domain, attributable to the size of the sulfur particles and to the absence of sulfur in the upper cloud. Also, the large sulfur particle model is clearly compatible with the polarization constraint, and prior calculations indicate that it can explain the different wavelength characteristics of albedo and contrast (*2*). The most serious problem that this model faces is its incompatibility with the shape of the net flux curve of Fig. 4 (*8*). Also, this model predicts too sharp a gradient in the UV intensity and ratio profiles above 54 km. Comparison of both sulfur models with this data implies that the UV absorber is present in the upper cloud region.

Sulfur dioxide looks promising. The spectral dependence of its absorption coefficient leads to a predicted albedo curve that is qualitatively similar to the observed curve. This model predicts a decrease in the net flux between 60 km and the cloud bottom that is comparable to the observed decrease, and it does predict some absorption above 55 km, although not enough. Also, it predicts an altitude dependence for the UV intensity and ratio of the UV to visible intensity that is similar to the observed profiles (Fig. 2). Better agreement could be achieved in these last two comparisons by increasing the optical depth above 62 km. The sharp increase in the mixing ratio of SO_2 with decreasing altitude in the upper parts of the cloud should lead to acceptable predictions for the wavelength dependence of contrast; in addition, there is no difficulty in fulfilling the polarization constraint. However, the SO_2 model does not produce a perfect match with the data: Its predicted albedo is too high in the 0.35- to 0.4-μm interval, and the shape seems wrong in the 0.4- to 0.45-μm interval. Also, it does not predict enough absorption above 0.4 μm in the upper part of the clouds. Conceivably, these problems are due to uncertainties attached to some of the parameters of SO_2 used in the calculations. In particular, the absorption coefficient of SO_2 is known only approximately at wavelengths longer than 0.32 μm (*22*). Future laboratory measurements will rectify this situation. In addition, large error bars are attached to the measured abundance of SO_2 in the lower atmosphere. Increases in either or both of these parameters would yield better agreement with the observations. At a minimum, it seems very likely that SO_2 absorption dominates Venus's spectrum at all wavelengths between 0.2 and 0.32 μm and plays some role at longer wavelengths.

Finally, suppose SO_2 is the UV absorber. The existence of dark and bright features would be due to variations in the mixing ratio of SO_2 in the upper parts of the clouds, where this ratio is decreasing rapidly because of photodissociation. Conceivably, dark areas are places of large-scale upward vertical motion or enhanced local turbulence, each of which would increase the amount of SO_2 in the upper cloud region (*25*).

JAMES B. POLLACK, BORIS RAGENT
ROBERT BOESE
NASA Ames Research Center, Moffett Field, California 94035
MARTIN G. TOMASKO
University of Arizona, Tucson 85721
JACQUES BLAMONT
Service d'Aeronomie du Centre National de la Recherche Scientifique, 91 Verrieres, France
ROBERT G. KNOLLENBERG
Particle Measuring Systems, Inc., Boulder, Colorado 80301
LARRY W. ESPOSITO, A. IAN STEWART
University of Colorado, Boulder 80309
LAWRENCE TRAVIS
NASA Goddard Institute for Space Studies, New York 10025

References and Notes

1. E. S. Barker, J. H. Woodman, M. A. Perry, *J. Atmos. Sci* **32**, 1205 (1975); L. Wallace, J. J. Caldwell, B. D. Savage, *Astrophys. J.* **172**, 755 (1972).
2. A. T. Young, *Icarus* **32**, 1 (1977).
3. G. T. Sill, *Commun. Lunar Planet. Lab.* **9**, 191 (1972); A. T. Young, *Icarus* **18**, 564 (1973); J. B. Pollack, E. F. Erickson, F. C. Witteborn, C. Chackerian, Jr., A. L. Summers, W. Van Camp, B. J. Baldwin, G. C. Augason, L. J. Caroff, *ibid.* **23**, 8 (1974).
4. J. B. Pollack *et al.*, *Icarus* **34**, 28 (1978).
5. K. Palmer and D. Williams, *Appl. Opt.* **14**, 208 (1975).
6. B. Hapke and R. Nelson, *J. Atmos. Sci.* **32**, 1212 (1975).
7. J. Blamont and B. Ragent, *Science* **205**, 65 (1979).
8. M. G. Tomasko, L. R. Doose, P. H. Smith, *ibid.*, p. 80.
9. L. D. Travis *et al.*, *ibid.* **203**, 781 (1979).
10. L. W. Esposito, J. R. Winick, A. I. Stewart, *Geophys. Res. Lett.*, in press.
11. J. E. Hansen and J. Hovenier, *J. Atmos. Sci.* **31**, 1137 (1974); L. Travis, personal communication.
12. J. B. Pollack *et al.*, *J. Appl. Meteorol.* **15**, 247 (1976).
13. J. B. Pollack and J. N. Cuzzi, *Proc. Third Conf. Atmos. Radiation* (1978), p. 20.
14. R. G. Knollenberg and D. M. Hunten, *Science* **205**, 70 (1979).
15. A. J. Watson, T. M. Donahue, D. H. Stedman, in preparation.
16. W. E. Spear and A. R. Adams, *J. Phys. Chem. Solids* **27**, 281 (1966).
17. A. P. Lenham and D. M. Treherne, *Observatory* **86**, 36 (1966); J. T. Twitty and J. A. Weinman, *J. Appl. Meteorol.* **10**, 725 (1971).
18. D. R. Huffman, *Adv. Phys.* **26**, 130 (1977).
19. A. P. Lenham and D. M. Treherne, in *Optical Properties of Metals and Alloys*, F. Abele, Ed. (North-Holland, Amsterdam, 1966).
20. R. P. Turco, *Geophys. Surv.* **2**, 153 (1975).
21. P. Warneck, F. F. Marmo, J. O. Sullivan, *J. Chem. Phys.* **40**, 1132 (1964).
22. Preliminary values of the absorption coefficient of SO_2 in the wavelength range from 0.32 to 0.6 μm were obtained from transmission measurements made by R. Nanes of California State University at Fullerton. These measurements were made for path lengths of 0.87 and 6.9 m on SO_2 at 1-bar pressure and room temperature.
23. V. I. Oyama, G. C. Carle, F. Woeller, J. B. Pollack, *Science* **203**, 802 (1979).
24. Sulfuric acid might oxidize the iron contained in the meteoritic material to the ferric oxidation state. A cursory examination of the optical properties of this altered material indicates it may not be satisfactory, either, but further study of this model is needed.
25. Some evidence for associating dark UV features with regions of upward motion has been given by D. Crisp and A. T. Young, *Icarus* **35**, 182 (1978).
26. We are grateful to K. Bilsky, W. Van Camp, and B. Baldwin for help with the calculations.

15 May 1979